

MASTER COPY: PLEASE KEEP THIS "MEMORANDUM OF TRANSMITTAL" BLANK FOR REPRODUCTION PURPOSES. WHEN REPORTS ARE GENERATED UNDER THE ARO SPONSORSHIP, FORWARD A COMPLETED COPY OF THIS FORM WITH EACH REPORT SHIPMENT TO THE ARO. THIS WILL ASSURE PROPER IDENTIFICATION. NOT TO BE USED FOR INTERIM PROGRESS REPORTS; SEE PAGE 2 FOR INTERIM PROGRESS REPORT INSTRUCTIONS.

MEMORANDUM OF TRANSMITTAL

U.S. Army Research Office
ATTN: AMSRL-RO-BI (TR)
P.O. Box 12211
Research Triangle Park, NC 27709-2211

Reprint (Orig + 2 copies)

Technical Report (Orig + 2 copies)

Manuscript (1 copy)

Final Progress Report (Orig + 2 copies)

Related Materials, Abstracts, Theses (1 copy)

CONTRACT/GRANT NUMBER:

REPORT TITLE:

is forwarded for your information.

SUBMITTED FOR PUBLICATION TO (applicable only if report is manuscript):

Sincerely,

REPORT DOCUMENTATION PAGE

Form Approved
OMB NO. 0704-0188

Public Reporting burden for this collection of information is estimated to average 1 hour per response, including the time for reviewing instructions, searching existing data sources, gathering and maintaining the data needed, and completing and reviewing the collection of information. Send comment regarding this burden estimates or any other aspect of this collection of information, including suggestions for reducing this burden, to Washington Headquarters Services, Directorate for information Operations and Reports, 1215 Jefferson Davis Highway, Suite 1204, Arlington, VA 22202-4302, and to the Office of Management and Budget, Paperwork Reduction Project (0704-0188,) Washington, DC 20503.

1. AGENCY USE ONLY (Leave Blank)		2. REPORT DATE		3. REPORT TYPE AND DATES COVERED	
4. TITLE AND SUBTITLE				5. FUNDING NUMBERS	
6. AUTHOR(S)					
7. PERFORMING ORGANIZATION NAME(S) AND ADDRESS(ES)				8. PERFORMING ORGANIZATION REPORT NUMBER	
9. SPONSORING / MONITORING AGENCY NAME(S) AND ADDRESS(ES) U. S. Army Research Office P.O. Box 12211 Research Triangle Park, NC 27709-2211				10. SPONSORING / MONITORING AGENCY REPORT NUMBER	
11. SUPPLEMENTARY NOTES The views, opinions and/or findings contained in this report are those of the author(s) and should not be construed as an official Department of the Army position, policy or decision, unless so designated by other documentation.					
12 a. DISTRIBUTION / AVAILABILITY STATEMENT Approved for public release; distribution unlimited.				12 b. DISTRIBUTION CODE	
13. ABSTRACT (Maximum 200 words)					
14. SUBJECT TERMS				15. NUMBER OF PAGES	
				16. PRICE CODE	
17. SECURITY CLASSIFICATION OR REPORT UNCLASSIFIED		18. SECURITY CLASSIFICATION ON THIS PAGE UNCLASSIFIED		19. SECURITY CLASSIFICATION OF ABSTRACT UNCLASSIFIED	
				20. LIMITATION OF ABSTRACT UL	

NSN 7540-01-280-5500

Standard Form 298 (Rev.2-89)
Prescribed by ANSI Std. 239-18
298-102

Enclosure 1

Evaluation of MIMO Techniques in FH-MA *Ad Hoc* Networks

Kostas Stamatiou, John G. Proakis and James R. Zeidler

Department of Electrical & Computer Engineering

University of California San Diego, La Jolla, CA 92093-0407

Email: kostas@ucsd.edu, jproakis@cw.cw.ucsd.edu, zeidler@ucsd.edu

Abstract—We consider an *ad hoc* network where frequency hopping (FH), convolutional coding and multiple antennas are employed in order to combat fading and multiple access (MA) interference. The transmitters are distributed in space according to the Poisson distribution and the corresponding receivers are situated at a fixed distance. Under a channel model that accounts for Rayleigh fading and path-loss, we derive an approximation to the frame-error-probability (FEP). This is in turn used to obtain simple expressions for network metrics of interest, such as the *network throughput* and the *information efficiency*, previously introduced in the literature. A number of interesting observations is made with respect to how the aforementioned metrics are affected by the code diversity order, the choice of multiple-input multiple-output (MIMO) technique and the propagation exponent.

I. INTRODUCTION

The use of MIMO techniques in the single-user scenario or in multi-user scenarios where a certain infrastructure is present, i.e. the multiple-access or broadcast channel, has been widely studied in the literature (the reader is referred to [1] for a comprehensive overview and large list of references). It is less clear in what manner MIMO techniques should be employed in the context of *ad hoc* networks. The problem is even more challenging in that it is not obvious what *network metrics* should be defined in order to evaluate the impact of these techniques.

In this paper, as in [2], we consider a Poisson distributed network of transmitters (TXs), each independently transmitting to its corresponding receiver (RX) at a fixed distance. Slow FH takes place during the transmission of a frame and the MA interference in each dwell is regarded as noise at the RX of interest¹. As advocated in [3], convolutional coding and interleaving are employed to harness the available interference diversity within the frame/codeword. Even though not optimal, we regard this no-scheduling scenario, where the links act independently of each other, as one of practical importance.

In the setting described above, we evaluate the performance of different MIMO techniques that require channel state information at the RX, namely maximal-ratio-combining (MRC), orthogonal space-time block coding (OSTBC) and spatial

multiplexing (SM) via zero-forcing (ZF). An approximation to the FEP and hence the packet throughput is derived, that provides insight on how the choice of MIMO technique affects the performance. The network metrics that are considered are the network throughput (NT), defined here as the product (spatial density of TXs) \times (packet throughput), as well as the information efficiency (IE) [4]–[6], defined as (transmission distance) \times (packet throughput). The NT addresses the need to pack as many possible transmissions in space, while maintaining a desirable packet throughput. On the other hand, the IE captures the trade-off present in a multi-hop network (of which the network we are studying can be considered as a snapshot), where transmitting farther means a packet needs fewer hops to reach its final destination, however the amount of interference in the network is increased. The IE as a network metric is also examined in [7], [8], where the authors consider a FH system with Reed Solomon coding and differential unitary space-time modulation.

In two very similar optimization problems, we find the density that maximizes the NT, for a *given* transmission distance and the transmission distance that maximizes the IE, for a given density. The optimal NT and IE are then evaluated for each MIMO technique and different numbers of TX and RX antennas. It is found that selecting a MIMO technique depends on the chosen metric, the number of antennas and the propagation exponent. The trends observed are similar to those presented in [9], however, we arrive at them via a different analytical path.

The rest of the paper is organized as follows. In section II, the system model is presented in detail. Section III includes the performance analysis and section IV the optimization of the network metrics. Our numerical results and conclusions are presented in sections V and VI.

II. SYSTEM MODEL

A. General

The TXs are distributed in the plane according to a homogeneous Poisson process of density λ and each TX has a corresponding RX at distance R (see [2] for more on the justification of this model). Packets are transmitted from all TXs concurrently and in a synchronized manner. The bandwidth is divided into M sub-bands, which are available for FH during the transmission of the packet. FH achieves a

This work was supported by the UC Discovery Grant com04-10173 and MURI Grant W911NF-04-1-0224.

¹Slow FH in this case means that a certain number of symbols are transmitted in each dwell.

“thinning” of the density of TXs, which allows us to assume that, in each dwell, a new realization of a Poisson process of density λ/M is present. This modelling may accommodate a practical scenario where the locations of the interfering TXs are fixed. However they “appear” random due to the fact that a different set of them is active over each sub-band. The realizations of the thinned Poisson process can be considered independent as long as the code diversity order is sufficiently smaller than M .

The channel between each TX-RX pair over a sub-band comprises constant flat Rayleigh fading and path-loss according to the law r^{-b} , where $b > 2$ is the propagation exponent. The transmitted power from each antenna is the same across all TXs and equal to one. There are m_t antennas at the TX and m_r antennas at the RX and we generally assume that $m_r \geq m_t$. We also disregard additive noise, such that interference from concurrent transmissions is the only cause of bit errors.

The information bits of each packet² are encoded, interleaved and mapped to BPSK symbols, which are the input to the TX MIMO block. A vector (or matrix) of symbols is transmitted from the TX antenna array over a specific sub-band which changes randomly over time. At the RX, the output of the corresponding RX MIMO block (where knowledge of the fading coefficients and interference power is assumed) is fed to the de-interleaver and the decoder. The performance of the decoder is characterized by the FEP. In the following, each MIMO technique is examined separately, however, any common notation is only explained the first time it is introduced. If w is a complex Gaussian random variable (r.v.) with mean 0 and variance σ^2 , we write $w \sim \mathcal{CN}(0, \sigma^2)$.

B. MRC

For MRC, the output of the RX MIMO block is

$$r = R^{-\frac{b}{2}} \mathbf{h}^H \mathbf{h} x + \sum_n R_n^{-\frac{b}{2}} \mathbf{h}^H \mathbf{h}_n x_n,$$

where \mathbf{h} is the $m_r \times 1$ fading vector between the TX and RX and \mathbf{h}_n is the fading vector between the interfering TX n (denoted TX _{n}) and RX; R_n is the distance between TX _{n} and RX; x and x_n are the BPSK symbols transmitted by TX and TX _{n} .

The vector $\mathbf{v}_n = \mathbf{h}_n x_n$ is Gaussian with covariance matrix \mathbf{I} . Therefore, we can equivalently write

$$r = \sqrt{a}x + w, \quad (1)$$

where $a = \|\mathbf{h}\|^2$ is a central chi-square distributed r.v. with parameter 1/2 and $2m_r$ degrees of freedom and $w \sim \mathcal{CN}(0, R^b \sum_n R_n^{-b})$, given $\{R_n\}$.

C. OSTBC

The vector at the RX antenna array is

$$\mathbf{y} = R^{-\frac{b}{2}} \mathbf{H} \mathbf{X} + \sum_n R_n^{-\frac{b}{2}} \mathbf{H}_n \mathbf{X}_n,$$

where \mathbf{X} and \mathbf{X}_n are the $m_t \times P$ space-time codewords transmitted by TX and TX _{n} ($P \geq m_t$). The $m_t = P = 2$ case corresponds to the well known Alamouti code.

Given $\{R_n\}$, the matrix $\mathbf{W} = \sum_n R_n^{-\frac{b}{2}} \mathbf{H}_n \mathbf{X}_n$ has i.i.d. Gaussian entries with variance $m_t \sum_n R_n^{-b}$. The output of the space-time decoder is described by (1) where a is now a central chi-square distributed r.v. with parameter 1/2 and $2m_t m_r$ degrees of freedom and $w \sim \mathcal{CN}(0, m_t R^b \sum_n R_n^{-b})$.

D. SM

The received vector is

$$\mathbf{y} = R^{-\frac{b}{2}} \mathbf{H} \mathbf{x} + \sum_n R_n^{-\frac{b}{2}} \mathbf{H}_n \mathbf{x}_n,$$

where \mathbf{x} and \mathbf{x}_n are the vectors transmitted by TX and TX _{n} . If the number of independent streams is $m \leq m_t$, the output of the ZF detector is described by (1), where the degrees of freedom of a are $2(m_r - m + 1)$ (see [10]) and $w \sim \mathcal{CN}(0, m R^b \sum_n R_n^{-b})$.

III. PERFORMANCE ANALYSIS

The decoder decides that the codeword $\hat{\mathbf{x}} = \{\hat{x}_k\}$ was sent if

$$\hat{\mathbf{x}} = \arg \min_{\mathbf{x} \in \mathcal{X}} \left\{ \sum_{k=1}^{\lfloor L_i/R_c \rfloor} \frac{|r_k - \sqrt{a_k} x_k|^2}{z_k} \right\},$$

where \mathcal{X} is the set of all transmitted codewords, L_i is the number of information bits, R_c is the rate of the convolutional code and z_k is the power of the interference at time k . Under the maximum-likelihood (ML) criterion,³ the probability of a length- l error event of the code, P_l , is computed by [11]

$$P_l = \frac{1}{\pi} \int_0^{\frac{\pi}{2}} \left[\Phi_\gamma \left(\frac{1}{\sin^2 \theta} \right) \right]^l d\theta \quad (2)$$

where $\Phi_\gamma(s) = \mathbb{E} [e^{-as/z}]$, $s > 0$, is the moment generating function (mgf) of the r.v. $\gamma = a/z$ and l is the length of the error event. In (2), the assumption that $\{a_k, z_k\}$ are independent within the span of the error event is implicit. This assumption is based on the interleaving of the bits within the codeword and the fact that, due to hopping, it is likely that a different set of interferers is active in each dwell, provided that $L \ll M$.

If a is chi-squared with $2N$ degrees of freedom, then

$$\Phi_{\gamma|z}(s) = \mathbb{E}_{\gamma|z} [e^{-\frac{s}{z}\gamma}] = \left(1 + \frac{s}{z} \right)^{-N}. \quad (3)$$

Moreover, the pdf of $z = mR^b \sum_n R_n^{-b}$ for any $b > 2$ follows the α -stable model [4]

$$f(z) = \frac{1}{\pi z} \sum_{k=1}^{+\infty} \frac{\Gamma(\alpha k + 1)}{k!} \left(\frac{\pi \lambda_{\text{eff}} m^\alpha \Gamma(1 - \alpha)}{z^\alpha} \right)^k \cdot \sin k\pi(1 - \alpha) \quad (4)$$

³ML decoding requires knowledge of $\{a_k, z_k\}$. How this is obtained is beyond the scope of this paper.

²We use the terms packet, frame and codeword interchangeably.

for $z > 0$, where the *effective density* is defined as

$$\lambda_{\text{eff}} = \frac{\lambda\pi R^2}{M}$$

and $\alpha \triangleq 2/b$ is the characteristic exponent. The effective density is the average number of nodes in the transmission range, normalized by the number of frequencies.

A. Evaluation of $\Phi_\gamma(s)$ and FEP

Our objective is to evaluate the integral

$$\Phi_\gamma(s) = \int_0^{+\infty} f(z)\Phi_{\gamma|z}(s) dz. \quad (5)$$

The integral can be computed numerically for $\alpha \in (0,1)$, however, that provides little insight on how the performance depends on λ_{eff} , m and N . Examining (3), we observe that the average performance over z depends mainly on the tail of $f(z)$, i.e. where z obtains its larger values. Since the tail of $f(z)$ is dominated by the smaller order terms in (4), we approximate $f(z)$ only by the first term, i.e.

$$f(z) \simeq \pi\alpha\lambda_{\text{eff}}m^\alpha z^{-1-\alpha}, \quad (6)$$

having made use of the identities (see [12], p.946)

$$\begin{aligned} \Gamma(1-\alpha)\Gamma(\alpha) &= \frac{\pi}{\sin \pi\alpha} \\ \Gamma(1+\alpha) &= \alpha\Gamma(\alpha) \end{aligned}$$

Substituting (3) and (6) in (5) and using eq.3.194.3 in [12], we have

$$\Phi_\gamma(s) \simeq \pi\alpha\lambda_{\text{eff}}m^\alpha B(N-\alpha, \alpha)s^{-\alpha}, \quad (7)$$

where $B(x, y)$ is the beta function. Plugging (7) in (2), the following approximation to P_l is derived (see [12], p. 412)

$$\begin{aligned} \tilde{P}_l &= \frac{2^{2\alpha l-1}}{\pi} B(\alpha l + 1/2, \alpha l + 1/2) \\ &\cdot (\pi\alpha\lambda_{\text{eff}}m^\alpha B(N-\alpha, \alpha))^l. \end{aligned} \quad (8)$$

If the shortest error event of the code has length L , the FEP is upper-bounded by [13]

$$P_F = L_i \sum_{l=L, L+1, \dots} k_l P_l, \quad (9)$$

where k_l is the multiplicity of the error event of length l . If P_l is replaced by \tilde{P}_l , then an approximation to P_F , \tilde{P}_F , is also obtained. In fig.1, P_F (labelled “exact”) and \tilde{P}_F (labelled “approx”) are plotted vs. $1/\lambda_{\text{eff}}$ for two different rate 1/2 codes and values of N (m is set to 1 and $b = 4$, or $\alpha = 0.5$); encoder 1 (Enc1) has $L = 6$ and encoder 2 (Enc2) has $L = 8$ (for details on these codes, see [14]). In agreement with (8), for small λ_{eff} , the code diversity order L determines the *slope* of each curve, while N determines the *coding gain* with respect to the $N = 1$ curve. Note that (8) becomes more inaccurate as λ_{eff} increases.

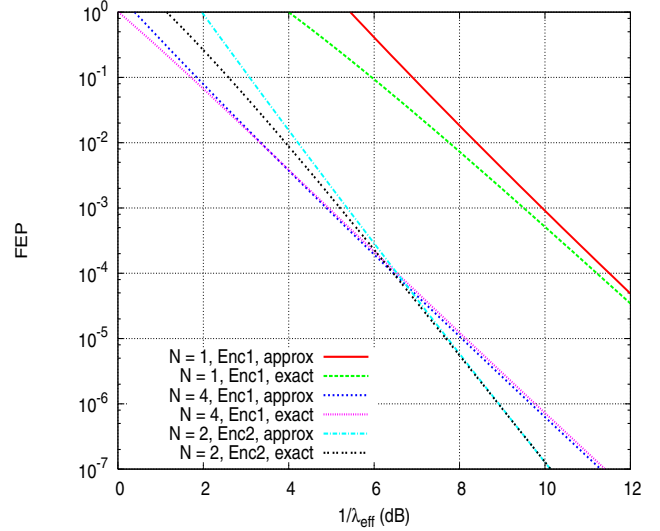


Fig. 1. FEP vs. $1/\lambda_{\text{eff}}$ for two different encoders ($m = 1$, $\alpha = 0.5$).

B. Asymptotics

From the definition of the beta function, we have that

$$B(N-\alpha, \alpha) = \Gamma(\alpha) \frac{\Gamma(N-\alpha)}{\Gamma(N)}.$$

For large x , $\Gamma(x) \sim \sqrt{2\pi}x^{x-1/2}e^{-x}$ ([12], p.945), so

$$\frac{\Gamma(N-\alpha)}{\Gamma(N)} \sim N^{-\alpha} \left(1 - \frac{\alpha}{N}\right)^{N-\alpha-\frac{1}{2}} e^{\alpha}.$$

However, it is easy to verify that

$$\lim_{N \rightarrow +\infty} \left(1 - \frac{\alpha}{N}\right)^{N-\alpha-\frac{1}{2}} = e^{-\alpha},$$

therefore

$$B(N-\alpha, \alpha) \sim \Gamma(\alpha)N^{-\alpha}. \quad (10)$$

We conclude that, for large N , the coding gain in fig.1 is proportional to $(N/m)^{-L\alpha}$.

IV. NETWORK METRICS

For a given R , we define the NT in b/s/Hz/m² as the product

$$\tau(\lambda) = \lambda(1 - P_F) \frac{R_M R_c}{M}, \quad (11)$$

where R_M is the information rate of the MIMO scheme, e.g. for the Alamouti code, it is $R_M = 1$, while for SM with m streams, it is $R_M = m$. Similarly, for a given λ , the IE (b/s/Hz \times m) is defined as

$$\eta(R) = R(1 - P_F) \frac{R_M R_c}{M}. \quad (12)$$

Since P_F is an increasing function of λ_{eff} , $\tau(\lambda)$ and $\eta(R)$ can be optimized over λ and R , respectively. In order to obtain some insight on where these maxima occur, we replace P_F with \tilde{P}_F in (11) and (12) and *ignore* all error events of length

$l > L$. Taking the derivatives over λ and R and setting them equal to zero, we easily find that

$$\tau_o = \lambda_o \left(1 - \frac{1}{L+1}\right) \frac{R_M R_c}{M} \quad (13)$$

$$\eta_o = R_o \left(1 - \frac{1}{2L+1}\right) \frac{R_M R_c}{M}. \quad (14)$$

The values of λ_o and R_o are

$$\lambda_o = f_1(L) \frac{M}{\pi R^2 m^\alpha \alpha B(N - \alpha, \alpha)}$$

$$R_o = f_2(L) \sqrt{\frac{M}{\pi \lambda m^\alpha \alpha B(N - \alpha, \alpha)}},$$

where

$$f_d(L) \frac{1}{dL} = \frac{2^{2\alpha L - 1}}{\pi} L_i k_L(dL + 1) B\left(\alpha L + \frac{1}{2}, \alpha L + \frac{1}{2}\right)$$

and $d = 1$ for τ_o , while $d = 2$ for η_o .

First, note that increasing the diversity order of the code has a multiplicative effect on τ_o and η_o through the factor

$$g_d(L) = f_d(L) \frac{dL}{dL + 1}.$$

It is straightforward to verify that $\lim_{L \rightarrow \infty} g_d(L) = 1$. Moreover, due to (10), as N increases

$$\tau_o \sim \left(\frac{N}{m}\right)^\alpha, \quad \eta_o \sim \left(\frac{N}{m}\right)^{\frac{\alpha}{2}}. \quad (15)$$

In the outage probability framework of [9], it was observed that the *transmission capacity* of the network also follows the trend of τ_o .

Based on (10), we can further optimize the NT or the IE over the number of streams m , when SM is employed. If NT is the metric of choice, then, setting $N = m_r - m + 1$ in (13), the function to be optimized is

$$\frac{g_1(L) R_c}{\pi R^2 \Gamma(1 + \alpha)} m \left(\frac{m_r - m + 1}{m}\right)^a.$$

Taking the derivative over m yields $m_{o,\tau} = (1 - a)(m_r + 1)$. Due to the constraints $m \in \mathcal{Z}^+$, $m \leq m_t$, we have

$$m_{o,\tau} = \min \{ \lceil (1 - \alpha)(m_r + 1) \rceil, m_t \}. \quad (16)$$

Similarly, the optimum number of streams, when IE is the network metric, is

$$m_{o,\eta} = \min \left\{ \left\lceil \left(1 - \frac{\alpha}{2}\right) (m_r + 1) \right\rceil, m_t \right\}. \quad (17)$$

V. NUMERICAL RESULTS

Unless otherwise stated, $L_i = 250$, $M = 100$, $\alpha = 0.5$. We consider the following MIMO scenarios: $1 \times m_r$ MRC, $2 \times m_r$ Alamouti and $m_r \times m_r$ SM, where $m = 2, m_o, m_r$ streams are activated (denoted as SM1, SM2 and SM3, respectively, for ease of exposition).

In fig.2, the NT corresponding to the performance curves of fig.1 is plotted vs. λ , for $R = 10m$. As pointed out earlier, since (8) becomes looser for larger λ_{eff} , the exact and

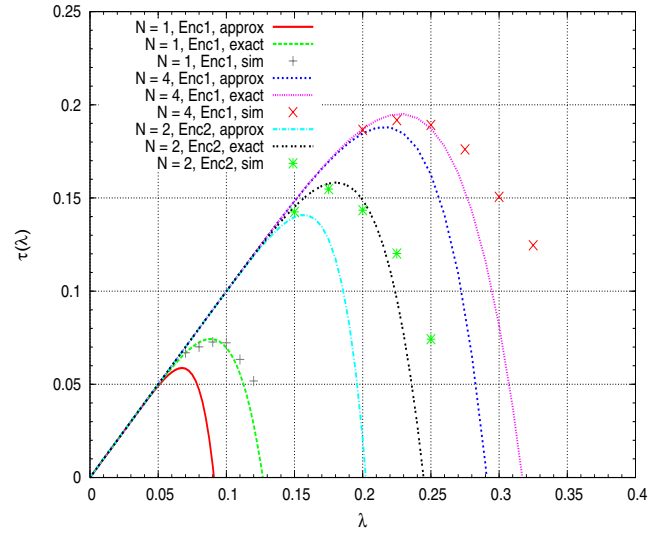


Fig. 2. NT vs. λ for two different encoders ($m = 1$ and $R = 10m$).

approximate curves diverge for increasing λ . The simulation points follow the exact curve up to a little after its maximum, then they begin to diverge. The explanation lies in the fact that (9) also becomes loose for increasing λ_{eff} . Also note that (13) gives quite accurate results, e.g. for Enc2 and $N = 2$, it yields $\tau_o \simeq 0.16$ and $\lambda_o \simeq 0.18$, values that agree with fig.2.

In fig.3, τ_o , normalized by $g_1(L) R_c / (\pi R^2)$, is plotted vs. m_r . The lowest τ_o is achieved by SM1. Also, the Alamouti code only slightly outperforms MRC; this is due to the fact that the increased spatial diversity order is obtained at the cost of increased interference, caused by the two independently transmitted streams, i.e. $(2m_r/2)^a = m_r^a$. Fig.3 also shows us that diversity techniques are preferable for small m_r ; as m_r increases, transmitting a number of independent streams pays off. Note that the fact that SM3 underlies SM2 at $m_r = 4$ is attributed to the inaccuracy of (10), for small N .

In fig.4, η_o , normalized by $g_2(L) R_c / \sqrt{M \pi \lambda}$, is plotted vs. m_r . The lowest η_o is now achieved by the diversity techniques. Due to the exponent $a/2$ in (15), the increase of m and thus the interference power is more than compensated for by the m -fold increase in rate, achieved by the SM schemes. As shown though by the gap between SM1 and SM3 curves, there is still a gain to be had if some of the streams are suppressed.

Finally, in fig.5, the dependency of τ_o on the propagation exponent is demonstrated, when $m_r = 6$. Looking at (15), it can roughly be said that, when the ratio N/m is larger than one, i.e. the useful signal power is larger than the interference power, a smaller b is preferable. This explains why τ_o decreases with b for all diversity techniques and SM2. In the case of SM1, the ratio is $1/m_r < 1$ and a larger b is preferable in order for the interference to be attenuated, hence the increase of τ_o with b .

VI. CONCLUDING REMARKS

We evaluated the performance of different single-user MIMO techniques in a FH-MA *ad hoc* network, where the

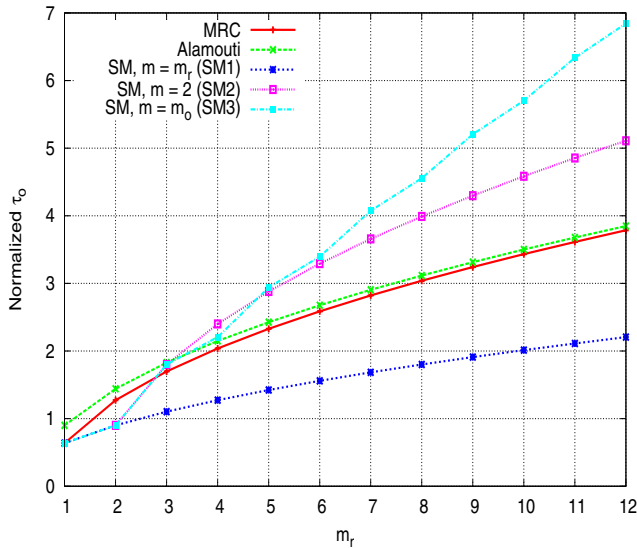


Fig. 3. Normalized τ_o vs. m_r for different MIMO modes.

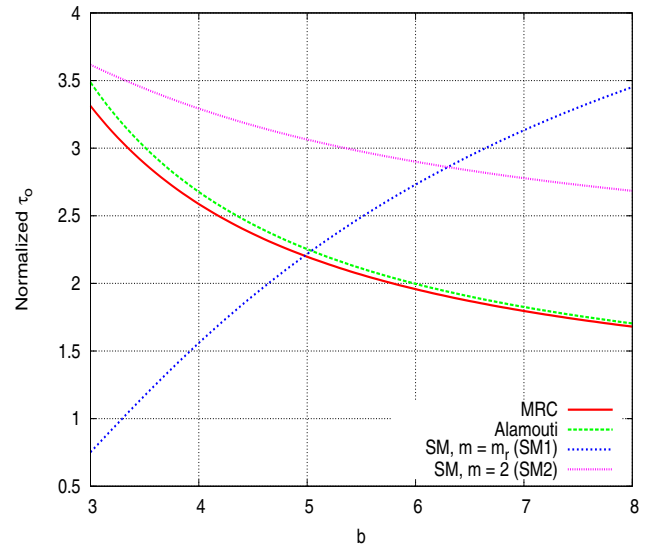


Fig. 5. Normalized τ_o vs. b for different MIMO modes and $m_r = 6$.

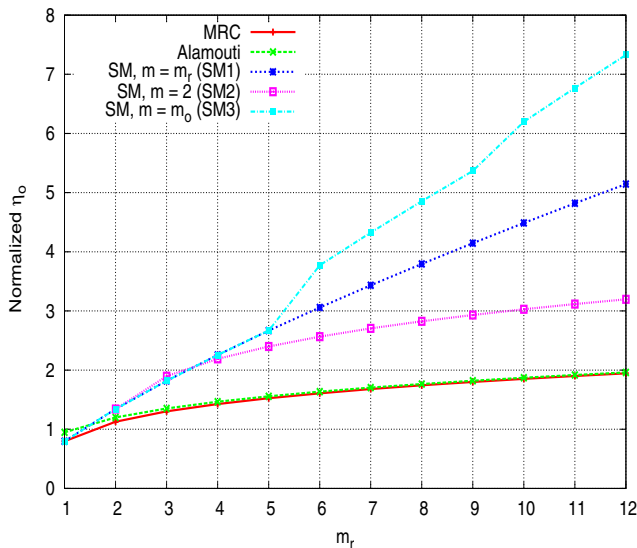


Fig. 4. Normalized η_o vs. m_r for different MIMO modes.

channel comprises fading and path loss and convolutional coding is employed for error protection. Our main conclusion is that the performance depends on the ratio of the available spatial diversity order over the number of independent streams, raised to the stability exponent α . In other words, any spatial diversity technique originally designed to provide diversity with respect to the fading, simply yields a power gain because of the nature of the α -stable interference.

The consequences of this trend on network metrics such as the NT and the IE were examined. It was observed that the best MIMO strategy depends on the choice of metric, the number of antennas and the propagation exponent. A useful byproduct of our analysis is the number of streams that must be active in SM mode, such that the desired metric is maximized. Future work will focus on how different MIMO techniques influence

network metrics that pertain to the multi-hop scenario, such as the spatial density of progress, introduced in [15].

REFERENCES

- [1] D. N. C. Tse and P. Viswanath, *Fundamentals of Wireless Communication*, 1st ed. Cambridge University Press, 2005.
- [2] S. P. Weber, X. Yang, J. G. Andrews, and G. de Veciana, "Transmission capacity of wireless ad hoc networks with outage constraints," *IEEE Trans. Inf. Theory*, vol. 51, pp. 4091–4102, Dec. 2005.
- [3] K. Stamatiou, J. G. Proakis, and J. R. Zeidler, "Information efficiency of ad hoc networks with FH-MIMO transceivers," in *Proc. IEEE ICC*, Jun. 2007.
- [4] E. S. Sousa and J. A. Silvester, "Optimum transmission ranges in a direct-sequence spread-spectrum multihop packet radio network," *IEEE J. Sel. Areas Commun.*, vol. 8, pp. 762–771, Jun. 1990.
- [5] M. W. Subbarao and B. L. Hughes, "Optimal transmission ranges and code rates for frequency-hop packet radio networks," *IEEE Trans. Commun.*, vol. 4, pp. 670–678, Apr. 2000.
- [6] M. R. Souryal, B. R. Vojcic, and R. L. Pickholtz, "Information efficiency of multihop packet radio networks with channel-adaptive routing," *IEEE J. Sel. Areas Commun.*, vol. 23, pp. 40–50, Jan. 2005.
- [7] H. Sui and J. R. Zeidler, "Information efficiency and transmission range optimization for coded MIMO FH-CDMA ad hoc networks in time-varying environment," 2007, *submitted to the IEEE Trans. on Comm.*
- [8] —, "Transmission range optimization for FH-CDMA networks in time-varying channels," *to appear in IEEE MILCOM 2007*.
- [9] A. M. Hunter, J. G. Andrews, and S. P. Weber, "Capacity scaling of ad hoc networks with spatial diversity," 2007, *submitted for publication*.
- [10] G. Caire, G. Taricco, J. V. Traveset, and E. Biglieri, "A multi-user approach to narrowband cellular communications," *IEEE Trans. Inf. Theory*, vol. 43, pp. 1503–1517, Sep. 1997.
- [11] M. K. Simon and D. Divsalar, "Some new twists to problems involving the Gaussian probability integral," *IEEE Trans. Commun.*, vol. 46, pp. 200–210, Feb. 1998.
- [12] I. S. Gradshteyn and I. M. Ryzhik, *Table of integrals, series and products*, 4th ed. Academic Press, 1994.
- [13] G. Caire and E. Viterbo, "Upper bound on the frame error probability of terminated trellis codes," *IEEE Commun. Lett.*, vol. 2, pp. 2–4, Jan. 1998.
- [14] M. L. Cedervall and R. Johannesson, "A fast algorithm for computing distance spectrum of convolutional codes," *IEEE Trans. Inf. Theory*, vol. 35, pp. 1146–1159, Nov. 1989.
- [15] F. Baccelli, B. Błaszczyszyn, and P. Mühlethaler, "An Aloha protocol for multi-hop mobile wireless networks," *IEEE Trans. Inf. Theory*, vol. 52, pp. 421–436, Feb. 2006.